PRAMANA
— journal of
physics

Vol. 72, No. 2
February 2009
pp. 303–314

Slow light with symmetric gap plasmon guides with finite width metal claddings

S DUTTA GUPTA
School of Physics, University of Hyderabad, Hyderabad 500 046, India
E-mail: sdgsp@uohyd.ernet.in

MS received 22 September 2008; revised 13 December 2008; accepted 2 January 2009

Abstract. We study the dispersion relation and the modes of a symmetric gap plasmon guide, where a dielectric planar slab is coated with finite metallic layers on both top and bottom. The finite conductivity of the metal is taken into account. The modes of the structure exhibit significant differences from those of dielectric waveguides with air or metal as the bounding media. Avoided level crossing phenomenon between the plasmon and the guided modes is shown to exist, leading to leaky modes. The structure sandwiched between two high index media is shown to lead to slow light in transmission. The group delay is shown to be larger for higher order modes.

Keywords. Gap plasmon; waveguide; slow light.

PACS Nos 42.82.Et; 73.40.Rw

1. Introduction

It is now well understood that the future of integrated optics depends very much on the realization of sub-wavelength devices [1]. Because of the Rayleigh limit, perhaps only the metal–dielectric structures offer the easiest possible solution for propagation of electromagnetic energy in such structures [2]. This along with the tremendous growth of technology of nanophotonics has led to the birth of plasmonics, an area where the potentials of surface plasmons [3] are exploited extensively. There have been many applications ranging from photon transport in nanostructures [2] and novel biosensing [4] devices to the possible realization of strong coupling regime of cavity quantum electrodynamics [5,6]. It has been shown that the fluorescence from a single molecule can be enhanced 20 times by a single metallic nanosphere [5]. Channeling of enhanced fluorescence by a nearby nanofibre has been demonstrated both theoretically and experimentally [7,8] opening up the avenues leading to atom probes and single photon sources. The possibility of entangling distant atoms by a nanofibre has also been pointed out [9]. A proposal to enhance the fluorescence of the atom by a nearby nanowire and coupling the radiation to the guided mode of a fibre was presented [6]. A phenomenal 95% efficiency was predicted.

Guiding structures (waveguides or fibres) with both metallic and dielectric constituents have been studied in detail [10–13] for quite some time. In the earlier studies, essentially a Drude-type model was used to describe the dispersion of metal. It was shown recently that the actual experimental data on dispersion of noble metals can lead to categorically different results as compared to the Drude model [14,15]. Very recently, the possibility of extremely large (sub-wavelength) confinement of the modes in metal–insulator–metal structures has been demonstrated [16]. The feasibility of broadband slow light is another interesting application of metal–dielectric guiding structures [17]. A great deal of research is now being devoted to the integration of plasmonic and dielectric structures [18]. Due to the complexity of the underlying structures, only extensive numerical methods like FDTD are shown to be effective for analysing such structures.

In the earlier days, the application of metal–dielectric structures were limited mainly to the polarizers for guided wave optics and various types of sensors [4,19]. Novel sensing applications based on the realization of a Mach–Zender interferometer have recently been demonstrated [20]. It was demonstrated that tapered structures can have very interesting applications like nanolensing and focusing of X-rays [21]. Recently, it was shown that tapered metal–dielectric–metal gap plasmon waveguides (GPW) can serve as the necessary interface between micro- (dielectric guide) and nano- (GPW) structures [22]. A transfer efficiency of about 70% from a 1.25 μm thick dielectric guide to a 50 nm GPW was demonstrated.

Most of the previous studies on GPW assumes semi-infinite metal claddings on both sides of the dielectric film [11,15,22]. The case of GPW with finite width metal cladding and their application for slow light has received little attention. In this paper, we present a detailed analysis of the modes of such a structure with special emphasis on the limiting cases when the outside medium is air or metal. We show that the dispersion curves corresponding to the last two cases can cross leading to the avoided crossing phenomenon of the dielectric guide with thin metal coatings. Analogous avoided crossing phenomenon has been reported in metal–dielectric microspheres [23]. Furthermore, we demonstrate the possibility of leaky modes [24], which can be excited by shining light directly on the structure. Such leaky modes have been studied in detail in the context of a finite Ag/silica/Ag guide [25]. Finally, we demonstrate the feasibility of slowing down light [26,27] in transmission through the structure. The finite transmission is mediated by the resonant tunneling through the structure, which acts as an effective symmetric barrier. We show that the higher-order modes can lead to larger delay. A delay of about 0.8 ps is demonstrated which corresponds to the enhancement of the free-space delay by about a factor of 26. Delay in such compact devices can be used to enhance the sensitivity of laser gyros and for many other purposes [28,29].

The organization of the paper is as follows. In §2 we present the derivation of the dispersion relation and the mode functions (only for TM modes, similar exercise can be carried out for the TE modes) for a symmetric layered medium for the sake of completeness, though there have been numerous other papers/monographs on similar transfer matrix approach [30]. We present the numerical results for the dispersion relation and the modes in §3. The same section contains the results on how these modes can be exploited for slowing down light. In conclusion, we summarize the main results.

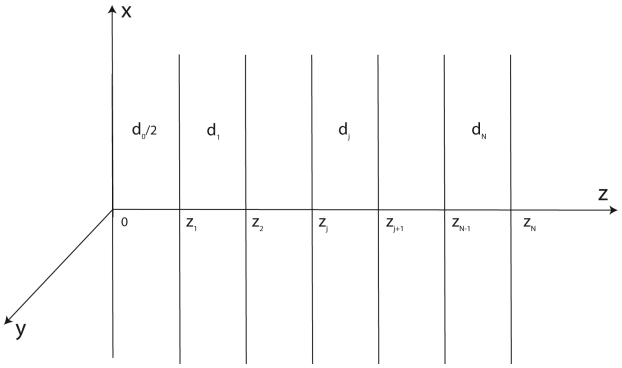

Figure 1. Schematic view of the symmetric layered medium, where only the right half is shown.

2. Dispersion relation and the modes of a symmetric $(2N + 1)$-layer waveguide

Consider the TM-modes (with non-vanishing components H_y, E_x and E_z) for the system shown in figure 1, comprising of $2N + 1$ layers with any jth layer characterized by a dielectric function $\varepsilon_j(\omega)$ and width d_j. The middle layer is assumed to have a width d_0 and dielectric function ε_0 (symbol not to be confused with the vacuum dielectric permittivity). Since noble metals are known to possess strong dispersion, we shall be incorporating available experimental data via suitable interpolation scheme like spline interpolation. The bounding media are assumed to be air. All the media are also assumed to be non-magnetic. Since we are interested in the propagation characteristics of the plasmonic modes we restrict our attention only to the TM polarized waves. For TM-polarized light the only non-vanishing magnetic field component is H_y, which for the jth layer can be written as

$$H_{jy} = A_{j+}\mathrm{e}^{ik_{jz}(z-z_j)} + A_{j-}\mathrm{e}^{-ik_{jz}(z-z_j)}, \quad j = 1, \ldots, N, \tag{1}$$

while the expression for the corresponding tangential component of the electric field E_{jx} is given by

$$E_{jx} = p_{jz}(A_{j+}\mathrm{e}^{ik_{jz}(z-z_j)} - A_{j-}\mathrm{e}^{-ik_{jz}(z-z_j)}). \tag{2}$$

In eqs (1) and (2), $A_{j\pm}$ are the forward and backward wave amplitudes, while k_{jz} and p_{jz} are expressed through the x-component of the propagation constant k_x as

$$k_{jz} = \sqrt{k_0^2\varepsilon_j - k_x^2}, \quad p_{jz} = \frac{k_{jz}}{k_0\varepsilon_j}, \quad k_0 = \frac{\omega}{c}. \tag{3}$$

In eq. (3) one has to ensure that the imaginary part of the z-component of the wave vector is positive. Writing eqs (1) and (2) on the left and right faces of the jth layer, one can relate the corresponding tangential field components by the matrix relation

$$\begin{pmatrix} H_y \\ E_x \end{pmatrix}_j = M_j \begin{pmatrix} H_y \\ E_x \end{pmatrix}_{j+1}, \tag{4}$$

where the subscript j refers to $z = z_j$ and the characteristic matrix M_j is given by [30]

$$M_j = \begin{pmatrix} \cos(k_{jz}d_j) & -(i/p_{jz})\sin(k_{jz}d_j) \\ -ip_{jz}\sin(k_{jz}d_j) & \cos(k_{jz}d_j) \end{pmatrix}. \tag{5}$$

Keeping in view the symmetry of the structure about the plane $z = 0$, we write the magnetic and electric field components in the central layer as

$$H_{0y} = A_0(\mathrm{e}^{ik_{0z}z} \pm \mathrm{e}^{-ik_{0z}z}), \tag{6}$$

$$E_{0x} = p_{0z}A_0(\mathrm{e}^{ik_{0z}z} \mp \mathrm{e}^{-ik_{0z}z}), \tag{7}$$

where $k_{0z} = \sqrt{k_0^2\varepsilon - k_x^2}$ and $p_{0z} = k_{0z}/k_0\varepsilon$. Hereafter the upper (lower) sign in eqs (6) and (7) will refer to the symmetric (antisymmetric) magnetic modes. Note that symmetry is being judged by the symmetry of the magnetic field distribution across the layers. Making use of the characteristic matrices one can then relate the tangential field components at the centre, i.e., at $z = 0$ and at $z = z_N$, which, in terms of amplitudes yields the following relation:

$$\begin{pmatrix} 1 & \pm 1 \\ p_{0z} & \mp p_{0z} \end{pmatrix} \begin{pmatrix} A_0 \\ A_0 \end{pmatrix} = M_T \begin{pmatrix} 1 \\ p_{tz} \end{pmatrix} A_t. \tag{8}$$

In eq. (8) the subscript t refers to the corresponding quantities in the embedding medium and M_T is given by

$$M_T = M_0(d_0/2)M_1(d_1)\cdots M_j(d_j)\cdots M_N(d_N). \tag{9}$$

Referring to the different signs in eq. (8) and demanding the non-triviality of the constant amplitudes, one obtains the dispersion relation for the symmetric and the antisymmetric modes. For the symmetric mode one has

$$m_{21} + m_{22}p_{tz} = 0, \tag{10}$$

$$(m_{11} + m_{12}p_{tz})A_t = 2A_0, \tag{11}$$

while for the antisymmetric mode one obtains

$$m_{11} + m_{12}p_{tz} = 0, \tag{12}$$

$$(m_{21} + m_{22}p_{tz})A_t = 2p_{0z}A_0. \tag{13}$$

It is clear that eqs (10) and (12) give the corresponding dispersion relations while (11) and (13) define the amplitudes for the mode functions.

We now restrict our attention to a symmetric metal clad waveguide with dielectric core thickness d_0, and metal claddings with width d_1. After the solution of the dispersion equations are obtained for complex k_x, the complete spatial dependence of the mode functions (for example, for the symmetric modes) in the various regions are given by:

For $z \leq d_0/2$

$$H_{0y}(x,z) = 2A_0 \cos(k_{0z}z)\mathrm{e}^{ik_x x}, \tag{14}$$

$$E_{0x}(x,z) = 2ip_{0z}A_0 \sin(k_{0z}z)\mathrm{e}^{ik_x x}, \tag{15}$$

$$E_{0z}(x,z) = -\frac{2A_0 k_x}{k_0\varepsilon}\cos(k_{0z}z)\mathrm{e}^{ik_x x}. \tag{16}$$

For $d_0/2 < z \leq d_0/2 + d_1$

$$H_{1y}(x,z) = (A_{1+}\mathrm{e}^{ik_{1z}(z-d_0/2)} + A_{1-}\mathrm{e}^{-ik_{1z}(z-d_0/2)})\mathrm{e}^{ik_x x}, \tag{17}$$

$$E_{1x}(x,z) = p_{1z}(A_{1+}\mathrm{e}^{ik_{1z}(z-d_0/2)} - A_{1-}\mathrm{e}^{-ik_{1z}(z-d_0/2)})\mathrm{e}^{ik_x x}, \tag{18}$$

$$E_{1z}(x,z) = -\frac{k_x}{k_0\varepsilon_1}(A_{1+}\mathrm{e}^{ik_{1z}(z-d_0/2)} + A_{1-}\mathrm{e}^{-ik_{1z}(z-d_0/2)})\mathrm{e}^{ik_x x}, \tag{19}$$

and for $z > d_0/2 + d_1$

$$H_{ty}(x,z) = A_t\mathrm{e}^{ik_{tz}(z-(d_0/2+d_1))}\mathrm{e}^{ik_x x}, \tag{20}$$

$$E_{tx}(x,z) = p_{tz}A_t\mathrm{e}^{ik_{tz}(z-(d_0/2+d_1))}\mathrm{e}^{ik_x x}, \tag{21}$$

$$E_{tz}(x,z) = -\frac{k_x}{k_0\varepsilon_t}A_t\mathrm{e}^{ik_{tz}(z-(d_0/2+d_1))}\mathrm{e}^{ik_x x}. \tag{22}$$

The constant A_t in eqs (20)–(22) are evaluated using (11), while $A_{1\pm}$ in eqs (17)–(19) are given by the solution of the following martix equation:

$$\begin{pmatrix} A_{1+} \\ A_{1-} \end{pmatrix} = \begin{pmatrix} \mathrm{e}^{ik_{1z}d_1} & \mathrm{e}^{-ik_{1z}d_1} \\ p_{1z}\mathrm{e}^{ik_{1z}d_1} & -p_{1z}\mathrm{e}^{-ik_{1z}d_1} \end{pmatrix}^{-1} \begin{pmatrix} 1 \\ p_{tz} \end{pmatrix} A_t. \tag{23}$$

The arbitrary constant A_0 is fixed by normalization of the modes. The power flow along the guide is given by the Poynting vector which can be written as follows:

$$P \sim \frac{1}{2}\mathrm{Re}\,(\vec{E}\times\vec{H}^*)\cdot\hat{n}_x = -\frac{1}{2}\mathrm{Re}\left[\left(-\frac{k_x}{k_0\varepsilon}H_y\right)(H_y^*)\right], \tag{24}$$

where both the complex fields contain full spatial dependence. Integrating over the transverse cross-section one obtains the normalization condition defining the

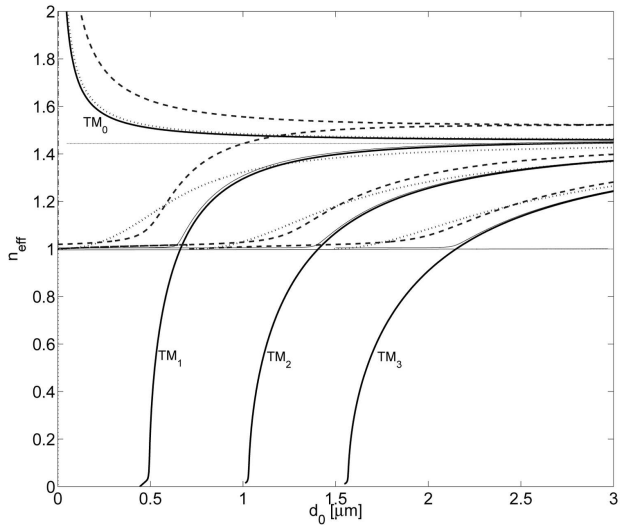

Figure 2. Solution of the dispersion relation for n_{eff} as functions of the core thickness d_0. The thick lines are for the semi-infinite metal claddings on the silica guide, the dotted lines are for the bare silica guide. The dashed lines are for the metal cladding thickness $d_1 = 0.01$ μm while the thin lines are for $d_1 = 0.03$ μm. The parameters are as follows: $\lambda = 1.55$ μm, $\varepsilon_0 = 2.085$, $\varepsilon_1 = -132 + 12.6i$, $\varepsilon_t = 1.0$. The leaky and the higher-order branches are not shown.

constant A_0. Assuming unit power input at $x = 0$, one can determine the constant A_0 using the following relation:

$$\int_0^{d_0/2} \mathrm{d}z\, \mathrm{Re}\left(\frac{k_x}{k_0\varepsilon}\right) |H_{0y}(z)|^2 + \int_{d_0/2}^{d_0/2+d_1} \mathrm{d}z\, \mathrm{Re}\left(\frac{k_x}{k_0\varepsilon_1}\right) |H_{1y}(z)|^2 + \int_{d_0/2+d_1}^{\infty} \mathrm{d}z\, \mathrm{Re}\left(\frac{k_x}{k_0\varepsilon_t}\right) |H_{ty}(z)|^2 = 1. \tag{25}$$

3. Numerical results and discussions

3.1 *Dispersion relation and mode functions*

In what follows, we present the results for the numerical calculations pertaining to the solutions of the dispersion equations (11) and (13), and the corresponding mode characteristics. For numerical calculation we chose the following parameters: $\lambda = 1.55$ μm, $\varepsilon_0 = 2.085$ (silica), $\varepsilon_1 = -132 + 12.6i$ (gold) [22], $\varepsilon_t = 1.0$ (air). We varied d_0 and d_1. The results for the dispersion are presented in figure 2, where we have plotted the effective index $n_{\text{eff}} = k_x/k_0$ as functions of d_0. We presented the results for both the symmetric and antisymmetric modes as well as

the plasmon and oscillating modes. For reference we have plotted the cases for (a) bare silica guide with outside medium as air (dotted lines) and (b) silica guide with semi-infinite metal claddings on both sides (thick lines). A comparison of the two cases reveal clearly that with metal cladding one can realize very low effective indices (close to zero) with the oscillatory modes, while the plasmon mode offers very large values. In contrast, the guided mode indices for the silica guide are limited in the range between air and silica refractive indices (i.e., between 1 and $\sqrt{2.085} = 1.44$). In the case of the GPW, one has the familiar splitting due to the coupling of the two interface plasmons. The uppermost branch (TM_0 plasmon) corresponds to the symmetric while the lower one to the antisymmetric oscillatory mode TM_1. We label the modes as plasmon (or oscillatory) depending on whether the magnetic field distribution inside the silica guide is expressible as a superposition of hyperbolic sine and cosine (or sines and cosines). Oscillatory modes from left to right are labelled by an increasing integer. It is clear from figure 2 that for semi-infinite metal claddings, there is a cut-off thickness for the oscillatory modes. For example, for $d \lesssim 0.5$ μm, there are no oscillatory modes with the realization of a single mode operation with just the TM_0 plasmon mode. However, the scenario changes drastically if one restricts the widths of the metal cladding. For example, for $d_1 = 0.01$ μm, the antisymmetric oscillatory mode exists which has a lower cut-off (see the dashed line). For a slightly larger thickness of the metal films, namely, $d_1 = 0.03$ μm, the behaviour almost coincides with the results for the guide with semi-infinite metal claddings. We have also studied the losses associated with the modes (not shown). Mode cut-off is determined by the sudden changes in the losses from small to large values as one reduces the gap width d_0. One also has the avoided crossing phenomenon like in coupled cavity–exciton systems. This, when the metal cladding thickness is very small, leads to the possibility of coupling of the surface plasmons on the two sides of the thin cladding layer. In other words, the surface plasmon on the metal/air interface can interact with the same on the other metal/silica interface. From a somewhat different angle, this phenomenon can be viewed as the crossing of the dispersion branches of an air/silica/air guide with that of the metal/silica/metal guide. The resulting level repulsion for finite width metal cladding is shown in figure 3. Indeed, the limiting cases are the bare silica guide and the gap plasmon guide with semi-infinite metal claddings. The case with finite and very low thickness of the metal cladding is in between and has the avoided crossing features. As expected, the avoided crossing effect is stronger for the lower thickness of the metal cladding. Note also that the value of the effective refractive indices for the modes corresponding to the part of the lower branches in figure 3 are less than unity. Thus these modes are leaky.

We next present the results for the mode functions. The modes are normalized as described previously using eq. (29). The results are presented in figure 4, where the top, middle and the bottom panels are for symmetric TM_0 mode of a silica guide in air, TM_0 plasmon and TM_2 oscillatory modes of a silica guide with gold coating with width $d_1 = 0.03$ μm, respectively. We emphasize the leaky mode nature of the TM_2 plasmon mode because of the fact that for this mode $\mathrm{Real}(n_{\mathrm{eff}}) < 1$ and the waves are of propagating character in the outside medium (air). However, since the corresponding z-component of the wave vector is complex in air (due to complex n_{eff}), the waves decay at very large distances away from the GPW.

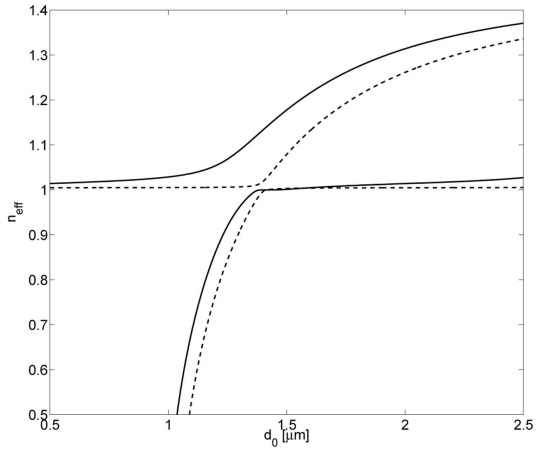

Figure 3. Avoided crossing phenomenon with the TM_2 mode. The solid (dashed) line is for $d_1 = 0.01$ μm ($d_1 = 0.03$ μm). Other parameters are as in figure 2.

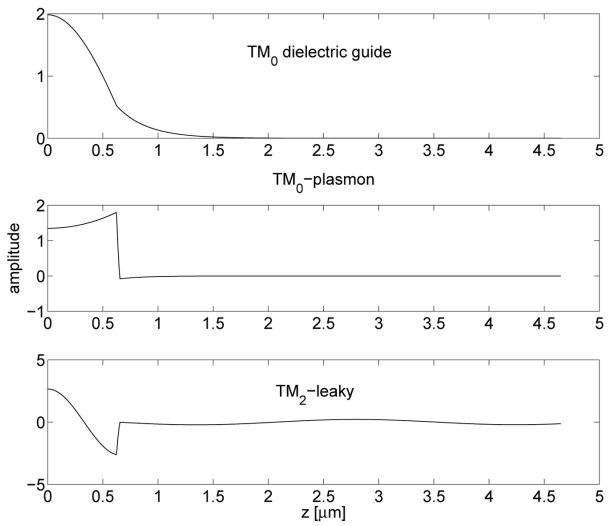

Figure 4. Real(H_y) as functions of transverse coordinate z for symmetric (top) TM_0 mode of a silica guide in air, (middle) TM_0 plasmon and (bottom) TM_2 oscillatory modes of a silica guide with gold coating with $d_0 = 1.25$ μm, $d_1 = 0.03$ μm. In view of symmetry we have shown the distributions only for half of the structure for $z \geq 0$.

3.2 *Slow light mediated by gap plasmon waveguides*

It was mentioned in the introduction that there are interesting applications of layered media for generation of slow light [27]. It was recently pointed out that sub-wavelength structures supporting surface plasmons can be exploited to generate broadband slow light [17]. In what follows we demonstrate that gap plasmon

structures can be used to generate slow light in transmission. We consider a three-layer gap plasmon structure as discussed earlier, except that the embedding media are now assumed to be dense with dielectric function $\varepsilon_t = 6.145$. Let a TM-polarized light be incident on the structure at an angle θ with the normal to the plane of stratification. It is clear that the transmission through the structure will be in general negligible because of the two metal films present. These two films along with the lower refractive index gap constitute the barrier, through which the tunnelling probability is small. However, with the excitation of the resonant modes of the structure there can be resonant tunnelling which may lead to finite transmission at the resonances. The delay through the structure can be calculated following Wigner [31]. This delay τ is given by the frequency derivative of the phase ϕ of the complex transmission coefficient

$$\tau = \frac{\partial \phi}{\partial \omega}, \tag{26}$$

which is to be evaluated at the pulse carrier frequency. It is understood that the pulse is assumed to have a narrow spectral band, failing which the distortions can be significant. The results for the intensity transmission coefficient T (top panel) and the delay τ (bottom panel) for $d_0 = 3.0$ and 5.0 μm, are shown in figures 5 and 6, respectively. It is clear from a comparison of figures 5 and 2 that the angular locations of the modes satisfy the following relation:

$$\sqrt{\varepsilon_f}\sin\theta \sim n_{\text{eff}}. \tag{27}$$

The bottom panels of figures 5 and 6 reveal that the delay is larger for the higher-order modes, which can be easily explained by the dispersion behaviour. In fact, the slope of the effective index as functions of frequency (not shown) is larger for higher-order modes leading to larger group index. At the same time losses are

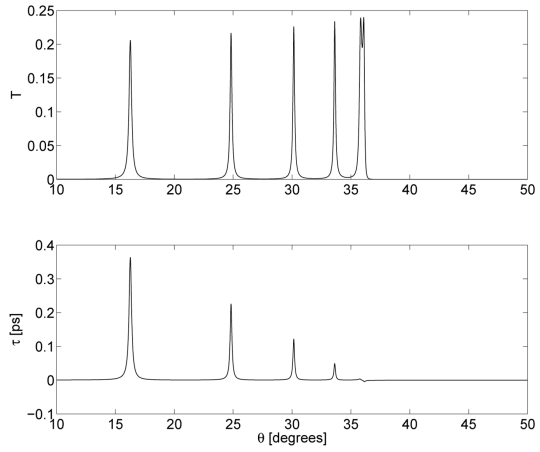

Figure 5. (Top) Intensity transmission coefficient T and (bottom) the Wigner delay τ as functions of the angle of incidence θ for $d_0 = 3.0$ μm, $d_1 = 0.03$ μm, $\varepsilon_t = 6.145$. The other parameters are as in figure 2.

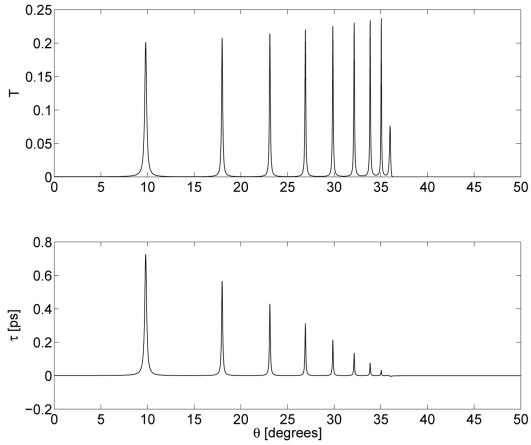

Figure 6. Same as in figure 5, except that now $d_0 = 5.0$ μm.

higher for higher-order modes. Thus working with higher-order modes leads to larger delay, albeit with slightly lower transmission. Note that for $d_0 = 3$ μm and for air as outside medium the only possible leaky mode is the TM_4 mode.

It may be noted that our calculations do not exhibit very high transmission, which may limit the applications of such GPW structures. However, the transmission coefficient for a given mode can be increased by adjusting (mostly reducing) the metal layer thickness, or by introducing additional two spacer layers (say, low index dielectric) on top and bottom of the GPW. The efficiency of coupling of the incident radiation to a given mode of the GPW, will crucially depend on the thickness of the metal and the spacer layer. The better the coupling efficiency, the higher will be the resonant tunnelling leading to higher transmission. It is also important to note that due to losses in metal, total transmission, even at discrete mode frequencies, is never possible.

4. Conclusions

In conclusion, we studied gap plasmon guides with thin metal claddings. Exact results for the dispersion relation for both the symmetric and antisymmetric modes were derived and analysed numerically. The dispersion curves exhibit marked differences from the limiting cases of dielectric guides with air or metal as the bounding media. Avoided level crossing phenomenon is also demonstrated. The gap plasmon guide with finite metal coating is shown to support leaky modes, which can be excited by direct illumination of the structure. Moreover, we show that slow light can be realized in transmission through such structures. The group delay, and hence, the group index is shown to be larger for higher-order modes.

Acknowledgement

This research was supported partly by a CSIR grant and partly by the Nano Initiative Program of the University of Hyderabad.

References

[1] W L Barnes, A Dereux and T Ebbesen, *Nature (London)* **424**, 824 (2003)
[2] S A Mier, P G Kik, H A Atwater, S Meltzer, E Harel, E E Koel and A A Requicha, *Nature Mat.* **2**, 229 (2003)
[3] V M Agranovich and D L Mills (eds), *Surface polaritons* (North Holland, Amsterdam, 1982)
[4] J Homola, *Annal. Bioanan. Chem.* **377**, 528 (2003)
[5] Sergei Kuhn, Ulf Hakanson, Lavinia Rogobete and Vahid Sandoghdar, *Phys. Rev. Lett.* **97**, 017402 (2006)
[6] D E Chang, A S Sorensen, P R Hemmer and M D Lukin, *Phys. Rev. Lett.* **97**, 053002-1 (2006)
[7] Fam Le Kien, S Dutta Gupta, V I Balykin and K Hakuta, *Phys. Rev.* **A72**, 032509 (2005)
[8] K P Nayak, P N Melentiev, M Morinaga, Fam Le Kien, V I Balykin and K Hakuta, preprint, quant-ph/0610136 (submitted to PRL)
[9] Fam Le Kien, S Dutta Gupta, K P Nayak and K Hakuta, *Phys. Rev.* **A72**, 063815 (2005)
[10] E N Economou, *Phys. Rev.* **182**, 539 (1969)
I P Kaminow, W L Mammel and H P Weber, *Appl. Opt.* **12**, 396 (1974)
[11] B Prade, J Y Vinet and A Mysyrowicz, *Phys. Rev.* **B44**, 13556 (1991)
[12] Pierre Berini, *Phys. Rev.* **B61**, 10484 (2000)
[13] Ian Breukelaar, Robert Charbonneau and Pierre Berini, *Appl. Phys. Lett.* **88**, 051119-1 (2006)
[14] J A Dionne, L A Sweatlock, H A Atwater and A Polman, *Phys. Rev.* **B72**, 075405-1, (2005)
[15] J A Dionne, L A Sweatlock, H A Atwater and A Polman, *Phys. Rev.* **B73**, 035407-1, (2006)
[16] Rashid Zia, Mark D Selker, Peter B Catrysse and Mark L Brongersma, *J. Opt. Soc. Am.* **A21**, 2442 (2004)
[17] Aristeidis Karalis, E Lidorikis, Mihai Ibanescu, J D Joannopoulos and Marin Soljacic, *Phys. Rev. Lett.* **95**, 063901 (2005)
[18] Michael Hochberg, Tom Baehr-Jones, Chris Walker and Axel Scherer, *Opt. Express* **12**, 5481 (2004)
[19] Dharmendra Kumar, V K Sharma and K N Tripathi, *Opt. Engg.* **45**, 054601 (2006)
P S Davids, B A Block and K C Kadien, *Opt. Express* **13**, 7063 (2005)
[20] Peter Debackere, Stijn Scheerlinck, Peter Bienstman and Roel Baets, *Opt. Express* **14**, 7063 (2006)
[21] C Bergemann, H Keymeulen and J F van der Veen, *Phys. Rev. Lett.* **91**, 204801-1 (2003)
[22] Pavel Ginzburg, David Arbel and Meir Orenstein, *Opt. Lett.* **31**, 3288 (2006)
[23] C Rohde, K Hasegawa and M Deutsch, *Opt. Lett.* **32**, 415 (2007)
[24] Rashid Zia, Mark D Selker and Mark L Brongersma, *Phys. Rev.* **B71**, 165431-1 (2005)

[25] J Chen, G A Smolyakov, S R J Brueck and K J Malloy, *Opt. Express* **16**, 14902 (2008)
[26] R W Boyd and D J Gauthier, Fast and Slow light, in: *Progress in optics* edited by E Wolf (Elsevier Science, Amsterdam, 2002), Vol. 43, pp. 497–530
[27] V S C Manga Rao, S Dutta Gupta and G S Agarwal, *Opt. Lett.* **29**, 307 (2004)
M Kulkarni, N Seshadri, V S C Manga Rao and S Dutta Gupta, *J. Mod. Opt.* **51**, 549 (2004)
V S C Manga Rao and S Dutta Gupta, *J. Opt. A: Pure and Appl. Opt.* **6**, 756 (2004)
[28] U Leonhardt and P Piwnicki, *Phys. Rev.* **A62**, 055801 (2000)
[29] Joe T Mok and Benjamin J Eggleton, *Nature (London)* **433**, 811 (2005)
[30] M Born and E Wolf, *Principles of optics* (Pergamon, New York, 1980), Chap. 1.6
[31] E P Wigner, *Phys. Rev.* **98**, 145 (1955)